Journal of Catalysis 262 (2009) 102–110

Contents lists available at ScienceDirect

Journal of Catalysis

www.elsevier.com/locate/jcat

In situ EXAFS and FTIR studies of the promotion behavior of Pt–Nb_2O_5/Al_2O_3 catalysts during the preferential oxidation of CO

S. Guerrero [a], J.T. Miller [b,c], A.J. Kropf [c], E.E. Wolf [a,*]

[a] *Chemical Engineering Department, University of Notre Dame, Notre Dame, IN 46556, USA*
[b] *BP Research Center, E-1F, 150 W. Warrenville Rd., Naperville, IL 60563, USA*
[c] *Chemical Engineering Division, Argonne National Laboratory, 9700 S. Cass Avenue, IL 60439, USA*

ARTICLE INFO

Article history:
Received 27 September 2008
Revised 8 December 2008
Accepted 9 December 2008
Available online 7 January 2009

Keywords:
PROX reaction
Pt supported catalyst
Nb promoter

ABSTRACT

The promotional effect of Nb to Pt/Al_2O_3 supported catalysts during the preferential oxidation of CO (PROX) was studied using various spectroscopic techniques. Addition of small amounts of Nb (<5%) stabilizes 40% of the loaded platinum as Pt^{2+}, which remains oxidized even after reduction treatments. This Nb-promoted catalyst is very active and selective for the PROX reaction. On Pt/Nb_2O_5 and at high Nb loading for the Pt/Nb/Al_2O_3 catalysts, the selectivity to CO_2 decreases and the selectivity for H_2 oxidation increases opposite to the selectivity observed at low Nb loadings. The increase CO_2 selectivity due to Nb promotion is ascribed to the inhibition of CO at low temperature which decreases hydrogen oxidation. *Operando* FTIR results indicate the presence of adsorbed CO as well as carbonates, bicarbonates and formates during the PROX reaction. An IR band at 968 cm^{-1} indicates the presence of Nb=O moieties at low Nb loadings. At higher Nb loadings, IR suggests the formation of three-dimensional Nb_2O_5 aggregates. The surface of the Nb containing catalysts is complex containing reduced and oxidized Pt which is modified by NbO_x species either surrounding the Pt crystallites or decorating them.

1. Introduction

The increased demand for fossil fuels have led to a renewed interest in alternative fuels, among them, the use of proton exchange membrane (PEM) fuel cells, utilizing hydrogen as energy source. The use of an upstream reformer of a hydrocarbon, such as methanol or ethanol, is among several processes investigated to produce hydrogen for PEM fuel cells. Such processes can provide a H_2-rich stream having an approximate composition of 45–75% H_2, 15–25% CO_2, 0.5–2% CO, 10–20% H_2O and N_2 [1,2]. The presence of CO in the reformer effluent stream, however, constitutes a problem since it acts as a poison of Pt used on the anode of the fuel cell, which requires reducing the CO concentration in the effluent below 20 ppm. This can be achieved by preferentially oxidizing CO to CO_2 in a H_2-rich stream upstream the fuel cell. The preferential oxidation of CO (PROX) requires highly selective catalyst for CO oxidation and at the same time unselective to the unwanted oxidation of H_2.

Pt is known for being an active catalyst in the PROX reaction [3–10] as it was first reported for such reaction to purify hydrogen used in ammonia synthesis [11]. Fuel cells, however, already utilize significant amounts of Pt, and therefore the Pt loading must be minimized in a PROX catalyst. One alternative is to use promoters that allow decreasing Pt loading while maintaining high activity and selectivity. Previous works have shown that combining Pt and Sn supported on a carbon support resulted in a better PROX activity than on an unpromoted Pt/Al_2O_3 catalyst [6,12]. This effect was attributed to the promotion of oxygen adsorption on Sn sites and to the competing adsorption of CO and H_2 on Pt sites [6]. It has also been suggested that promoters can positively affect the catalyst selectivity by blocking the spillover of adsorbed oxygen onto the support and/or hydrogen species, both involved in hydrogen oxidation [10,13–15]. Minemura et al. [16] reported that during the PROX reaction, a 2% Pt supported on Al_2O_3 promoted with potassium could reach 100% CO conversion and 50% CO_2 selectivity at around 90 °C.

In a previous paper [17], we reported an interesting promotion–inhibition effect of adding Nb to Al_2O_3-supported Pt catalysts during the PROX reaction. At low Nb loadings the catalysts were very active and selective for CO oxidation. As Nb loading increased, this effect reversed and in the limit of Nb loading, i.e. Pt supported on niobia, the CO selectivity of Pt was inhibited during the PROX reaction. Interestingly, this latter catalyst is very active for hydrogen oxidation in the presence of significant amounts of CO, i.e. it becomes resistant to CO poisoning.

In this work, we present *in situ* and *operando* (under reaction conditions) FTIR and EXAFS/XANES spectroscopy characterization

* Corresponding author. Fax: +1 574 631 8366.
E-mail address: ewolf@nd.edu (E.E. Wolf).

0021-9517/$ – see front matter
doi:10.1016/j.jcat.2008.12.008

results from Pt/Nb/Al_2O_3 catalysts using various Nb loadings to explain the promotion–inhibition effect previously reported.

2. Experimental

2.1. Catalysts preparation

Several methods of catalyst preparation were used to add Nb to the Al_2O_3 support, but the results proved to be independent of the way Nb was loaded [17]. In all cases, Pt was loaded onto Nb containing supports by incipient wetness impregnation using tetraammineplatinum(II) nitrate (Aldrich) followed by calcination in air at 300 °C for 4 h. Initially, Nb was loaded on the Al_2O_3 support (X%Nb–Al_2O_3, X = 0, 1, 5, 10, 20 is the niobium loading) by co-precipitation of ammonium niobium oxalate (Aldrich) and colloidal alumina sol (Criterion Catalyst and Technologies) with aqueous ammonia. These supports were calcined at 500 °C for 12 h. Catalysts were also prepared by impregnation of Al_2O_3 with Nb oxalate followed by calcination at 300 °C for 2 h. Catalysts with Nb loading lower than 20% are referred as low Nb loading. Higher loadings of Nb of 30 and 50% (1%Pt/Y%Nb–Al_2O_3, Y = 30, 50) were attained by the successive impregnation of Nb using ammonium niobium oxalate followed by impregnation of tetraammineplatinum(II) nitrate and calcination at 300 °C for 4 h. The Nb_2O_5, used as support for the 1%Pt/Nb_2O_5 catalyst, was prepared by a microemulsion of a solution of ammonium niobium oxalate diluted in 10 g of pluronic acid L64 (BASF), which was strongly stirred until the formation of a foam was observed. Precipitation of Nb_2O_5 was induced by adding a solution of NH_4OH, 0.5 M (100 ml) to the foam. After filtration, the solid was washed with ethanol and the remaining solvent was extracted from the solid by using boiling acetone. After drying overnight at room temperature, the resulting solid was calcined at 300 °C for 2 h.

2.2. Activity-selectivity measurements

Catalysts' activity was measured in a quartz tubular flow reactor of 1 cm ID and 30 cm long, using 200 mg of catalyst. The catalyst powders were first pelletized and the resulting pellets broken up into a powder that was sieved to yield agglomerates with average particle sizes of about 1 mm. The reactants flow rates were kept constant by electronic mass flow controllers. A temperature controller, using a feedback from a thermocouple placed in a thermo-well located in the center of the catalyst bed, controlled an electrical heater and maintained the reactor temperature constant (±0.1 °C). The reactor is also equipped with an external diaphragm pump (Thomas Industries) to provide an external recycle loop. The recycle ratio (recycled flow rate/outlet flow rate) was about 20 to ensure conditions equivalent to perfect mixing and to eliminate diffusional mass and heat-transport effects during reaction. The perfect mixing conditions allowed the direct calculation of reaction rates in a much broader range of reaction conditions (up to 100% conversion) that cannot be attained under differential reaction conditions normally used in single pass plug flow reactors (i.e. at less than 10% conversion).

Prior to each run, the catalysts were reduced *in situ* at 200 °C in a stream of pure hydrogen flowing at 50 cc/min for 1 h. When higher reduction temperatures were used, the same activity results were obtained. After cooling the reactor to room temperature and purging with helium, the reaction mixture with a composition of 0.8% CO, 0.8% O_2, and 51% H_2, with He as balance, was added at a total flow rate of 195 cc/min. Experiments were conducted by increasing linearly the reactor temperature at 1 °C/min until reaching 200 °C.

Samples from the gaseous effluent were analyzed on stream using a gas chromatograph (Varian 3700) equipped with a CTR I (Alltech) and a molecular sieve (Alltech) columns, operating in parallel, and maintained at 50 °C using He as a carrier at 120 cc/min. This column arrangement allows separating H_2, CO, O_2, CO_2, and CH_4. The latter gas was not detected in any experiment. Selectivity is defined as the ratio between oxygen consumed in the oxidation of CO versus the total amount of oxygen consumed and it was calculated as: $S_e = P^{out}_{co2}/2(P^{in}_{o2} - P^{out}_{o2})$, where P_i corresponds to the partial pressure of the component i.

2.3. FTIR measurements

IR measurements were obtained in both transmission and diffuse reflectance mode (DRIFTS). Transmission infrared spectra of pressed disks (~20 mg) were collected *in situ* in an IR reactor cell placed in a Mattson FTIR spectrometer (Galaxy 6020). Data were recorded at a resolution of 2 cm^{-1} and 30 scans per spectrum. The IR cell is equipped with CsI windows, and has connections for inlet and outlet gas flows, and has two thermocouples connected to a temperature controller to monitor and control the cell and catalyst temperature. Spectra were recorded in absorbance mode after subtraction of the background spectrum of the catalyst's disk under helium at the corresponding temperature. The samples were pretreated at various conditions prior to study adsorption and reaction. After pretreatment, the catalyst was cooled to room temperature in He, and under *operando* or reaction conditions, the reaction mixture was introduced in the cell at a total flow rate of 195 cc/min and a composition of 0.8% CO, 0.8% O_2, and 51% H_2, with He as balance. Spectra were collected at different temperatures as it increased at a rate of 1 °C/min. Transmission experiments in which no reaction was carried out (i.e. *in situ*), such as CO adsorption and desorption, showed different intensities and frequencies than under reaction or *operando* conditions and thus are not shown.

The DRIFTS experiments were carried out to obtain spectra at low frequencies related to support species which could not be obtained under transmission mode. DRIFTS results were obtained in a special IR reaction cell equipped with ZnSe windows and a praying mantis optical geometry (Harrick, 3-3S) placed in a Bruker FTIR spectrometer (Equinox 55). The cell includes a heating element and a thermocouple, which provides the feedback to a temperature controller to maintain the temperature constant at a set value. The gases flow upwards through a shallow bed of catalysts reaching the dome of the cell and flowing out near its base. A total of 250 scans were recorded per spectrum, which was displayed in Kubelka–Munk units, over the range of 4000–500 cm^{-1} at a resolution of 2 cm^{-1}. To improve the reflectivity of the samples, the catalysts were diluted with KBr at ratio of KBr:catalyst of 10:1. In every experiment, 50 milligrams of catalysts sample were reduced in 15 cc/min of H_2 at 200 °C for 1 h. Pure KBr was used as background after the same conditions of the reduction pretreatment were used, which was then subtracted from the IR spectrum of the sample to correct for temperature effects.

2.4. EXAFS data collection and analysis

Measurements using extended X-ray absorption fine-structure (EXAFS) spectroscopy were made on the insertion-device beam line at the advanced photon source (APS), Argonne National Laboratory (ANL). Measurements were made in transmission mode with ionization chambers optimized for the maximum current with linear response (~10^{10} photons detected/s). A cryogenically cooled double-crystal Si (111) monochromator with resolution (ΔE) better than 2.5 eV at 13272.6 keV (Pt L_2 edge) was used in conjunction with a Rh-coated mirror to minimize the presence of harmonics [18]. The integration time per data point was 1–3 s, and three

scans were obtained for each processing condition. Standard procedures based on WINXAS97 software [19] were used to extract the EXAFS results [20]. Phase shifts and backscattering amplitudes were obtained from EXAFS results using $Na_2Pt(OH)_6$ as a reference compound for Pt–O parameters and a Pt foil for Pt–Pt parameters.

The sample was pressed into a cylindrical holder with a thickness chosen to give an absorbance ($\Delta\mu x$) of about 1.0 in the Pt edge region, corresponding to approximately 30 mg of catalyst. The sample holder was centered in a continuous-flow *in situ* EXAFS reactor tube (18 in. long, 0.75-in. diameter) fitted at both ends with polyimide windows and valves to isolate the reactor from the atmosphere. The catalysts were first reduced outside the EXAFS data acquisition room by flowing a mixture of 4%H_2/He. After the prescribed treatment the sample was cooled to room temperature in He, and then the cell was isolated by closing the valves fitted at both ends of the tube and moved to the EXAFS data acquisition room. Experiments were conducted *in situ* in a stream of either 1%CO/He or in 4%H_2/He at 110, 155, and 205 °C. As in the case of FTIR studies, results were obtained under various *in situ* and *operando* conditions. The later were carried out by flowing 200 cc/min of a mixture of 1%CO/He, 1%O_2/He, and 4%H_2/He, balance He, at 110, 155, and 205 °C and showed the effect of the reaction on the surface.

3. Results

3.1. Activity

Table 1 summarizes previous key activity results for selected catalysts and at conditions emphasizing the niobia promotion–inhibition behavior of the Pt supported catalysts. Details for other catalysts and conditions used are listed in [17]. In short, Pt promoted with low Nb loadings (5–20%) increased the PROX reaction activity and selectivity, and as loading increased, the activity-selectivity resembled the unpromoted catalyst. When Pt was supported on Nb_2O_5 however, the PROX activity was inhibited significantly. Also listed in Table 1 are the conversion for CO oxidation and hydrogen oxidation only, the later reaction being the fastest one reaching 100% conversion at room temperature. CO oxidation on Pt/Nb_2O_5, however, exhibited high activity when hydrogen was not present in the feed, albeit lower than on Pt supported on alumina with or without niobia. Table 1 also lists the Pt dispersion (D) for each catalyst showing that the Pt/Nb_2O_5 catalyst has smaller Pt dispersion than that of the unpromoted and Nb promoted Pt/Al_2O_3 catalysts.

Table 1
Conversion and selectivity for the PROX reaction on selected catalysts. CO and H_2 oxidation only are also included.

Catalysts (D = dispersion)	Temp. (°C)	PROX		CO oxidation conversion (%)	H_2 oxidation conversion (%)
		CO conversion (%)	CO_2 selectivity (%)		
Pt/Al_2O_3 (74%D)	150	23	100	100	100
Pt/5%Nb–Al_2O_3 (74%D)	150	85	73	100	100
Pt/Nb_2O_5 (27%D)	150	5	5	23	100
	180	10	4	100	100

3.2. XAS characterization

The EXAFS and XANES data were obtained in various gases (CO, H_2 only as well as under PROX conditions) and at different temperatures on the 1%Pt/X%Nb–Al_2O_3 (X = 0, 1, 5, 10) catalysts. EXAFS fits of the k^2-weighted Fourier transform data are given in Table 2, for the unpromoted and reduced Pt/Al_2O_3, while fits for the 1%Pt/X%Nb–Al_2O_3 (X = 0, 1, 5, 10) catalysts reduced at 250 °C are presented in Table 3. Table 4 gives the results for the 1%Pt/5%Nb–Al_2O_3 catalyst reduced at different temperatures. For the unpromoted 1%Pt/Al_2O_3 catalyst (Table 2), the Pt–Pt scattering (bond) distance and coordination number (CN) remain approximately the same with the gas atmosphere (H_2, CO, PROX) or temperature used (25–205 °C). The Pt–Pt scattering distance values are slightly shorter than that for Pt foil (2.77 Å), which is consistent with the presence of small particles on the supported catalyst [21]. The absence of Pt–O during PROX reaction indicates that there is little Pt oxidation despite the presence of O_2 in the gas mixture. As it was previously reported using TEM, the particle size distribution for these catalysts is in the range of 10–20 Å [17].

XANES spectra of the reduced Pt/Al_2O_3 catalysts, in the presence or absence of CO at various temperatures, are shown in Fig. 1. The height of the Pt edge (white line) varies with the amount of adsorbed CO and with temperature (see inserts in Fig. 1). An approximate estimate of the corresponding CO coverage at different temperatures can be made by fitting a linear combination of the reduced (no CO) and CO-saturated Pt XANES white line [22,23]. The same procedure was used to fit the XANES spectra in hydrogen at different temperatures (Table 4) [24]. The XANES estimate of the percentage of CO saturation is also listed in Table 2.

Fig. 1A also shows the XANES spectra of the Pt/Al_2O_3 catalyst at 110, 155, and 205 °C in the presence of flowing CO. The white line intensity at 110 and 155 °C is very similar to that of a surface completely covered by CO (see Table 2). The white line intensity decreases slightly when the sample is heated to 205 °C in flowing CO, corresponding to an estimated decrease in CO coverage of about 85% of its saturation value. When the same experiment was repeated at 155 °C in 1% CO with 4% H_2/He (Table 2), the white line estimate indicated that CO decreased to about 65% of the saturation coverage, possibly due to competitive adsorption between H_2 and CO. The CO coverage estimate from the white line intensity on the unpromoted Pt/Al_2O_3 catalyst was also made under PROX

Table 2
EXAFS and XANES fits: 1%Pt/Al_2O_3 under various experimental conditions. Prior each experiment the catalyst was reduced at 250 °C in 4%H_2/He.

Conditions		CO saturation (%)	Scatter	CN (±10%)	R (Å) (±0.02)	$\Delta\sigma^2$ ($\times 10^3$ Å^2)	E_0 (eV)
Temperature (°C)	Gas[a]						
25	4% H_2	–	Pt–Pt	8.9	2.75	3.0	−4.2
110	4% H_2	–	Pt–Pt	8.9	2.74	3.4	−4.4
205	4% H_2	–	Pt–Pt	8.9	2.73	3.8	−4.2
110	1% CO	100	Pt–Pt	8.7	2.75	3.4	−3.8
155	1% CO	100	Pt–Pt	8.6	2.76	3.6	−3.7
155	1% CO + 4% H_2	65	CO desorbs in flowing H_2 at 155 °C				
205	1% CO	85	Pt–Pt	8.4	2.75	3.8	−3.9
110	0.8% CO + 0.8% O_2 + 4% H_2	100	Pt–Pt	9.0	2.76	3.4	−3.4
155	0.8% CO + 0.8% O_2 + 4% H_2	75	Pt–Pt	9.0	2.75	3.6	−4.3
205	0.8% CO + 0.8% O_2 + 4% H_2	55	Pt–Pt	9.2	2.75	3.8	−4.2

Table 3
EXAFS and XANES fits. 1%Pt/X%Nb–Al_2O_3 catalyst prereduced at 250 °C.

Pt/X%Nb–Al_2O_3 Nb loading, %	Fraction Pt^{2+}	Fraction Pt^0	Scatter	CN (±10%)	R (Å) (±0.02)	$\Delta\sigma^2$ ($\times10^3$ Å^2)	E_0 (eV)
0	–	1.0	Pt–Pt	8.9	2.75	3.0	−4.2
1	0.4	0.6	Pt–O	1.2	2.01	3.0	−2.0
			Pt–Pt	3.6	2.70	5.0	−6.6
5	0.4	0.6	Pt–O	1.1	2.00	3.0	−2.1
			Pt–Pt	4.3	2.71	5.0	−4.6
10	0.3	0.7	Pt–O	1.1	2.00	3.0	−2.0
			Pt–Pt	3.4	2.70	5.0	−5.2

Table 4
EXAFS and XANES fits on l%Pt/5%Nb–Al_2O_3. Data collected under He at 25, 110, and 205 °C right after reduction in 4% H_2 at the same temperatures.

Conditions		H_2 saturation (%)	Scatter	CN (±10%)	R (Å) (±0.02)	$\Delta\sigma^2$ ($\times10^3$ Å^2)	E_0 (eV)
Temperature (°C)	Gas						
25	4% H_2	100	Pt–O	2.0	2.04	3.1	−0.7
			Pt–Pt	3.9	2.71	6.3	−1.2
110	4% H_2	90	Pt–O	2.2	2.02	6.0	−3.7
			Pt–Pt	3.8	2.69	6.5	−6.0
205	4% H_2	0	Pt–O	2.0	2.01	7.9	−2.9
			Pt–Pt	4.0	2.69	5.0	−5.6
205	Air	–	Pt–O	3.8	2.04	0.2	−2.1

reaction conditions. Fig. 1B shows that under reaction conditions, the white line intensity decreases with temperature indicating that CO saturation gradually decreases when increasing temperature. When the reaction was carried out at 110 °C, the white line intensity corresponded to a surface completely saturated with CO (Table 2). A further increase in the reaction temperature to 155 °C led to an estimate of 75% of CO saturation coverage. The lowest CO saturation coverage estimate corresponded to 55% at 205 °C. These results indicate that, under reaction conditions CO coverage is lower than when only CO is present due to the competitive adsorption of CO, H_2, and oxygen. Fits of the EXAFS data indicate little change in the coordination number (CN) and scattering distance (R) between the reduced 1%Pt/Al_2O_3 with adsorbed CO or under PROX reaction at 205 °C. This indicates that the Pt particle size does not change with either flowing CO or under PROX reaction conditions and that the Pt remains fully metallic under reaction conditions and partial conversion.

Fig. 2A shows the XANES spectra for the Pt/X% Nb–Al_2O_3 (X = 0, 5, 10, 20) catalysts, i.e., those with low Nb loading. The results indicate that with low Nb loading Pt remains partially oxidized even after reduction in H_2 at 250 °C. Estimates made by fitting the normalized XANES indicate that the Pt/5%Nb–Al_2O_3 and Pt/10%Nb–Al_2O_3 catalysts are approximately 40% Pt^{2+} and 60% as Pt^0 (see Table 3). Similarly, for Pt/20%Nb–Al_2O_3, 30% of the platinum is Pt^{2+} and 70% is Pt^0. By contrast, the unpromoted Pt/Al_2O_3 catalyst is fully reduced metallic Pt. While only a portion of the Pt is reduced in H_2 at 250 °C for Pt/Nb–Al_2O_3 catalysts, air oxidation at 205 °C, leads to complete oxidation to PtO, i.e., Pt^{2+} (Fig. 2B). Fig. 3A shows that Pt L_{II} XANES intensity of Pt/5%Nb–Al_2O_3 increases upon CO adsorption at 110 °C. At 205 °C, the XANES intensity decreases to about 70% of the CO saturation coverage.

Under PROX reaction conditions at 110 °C, Fig. 3B, the XANES intensity is the same as with 100% CO coverage, i.e., pure CO (see Fig. 3A). At 155 °C there is a decrease in the white line intensity, and it is estimated as 80% of the CO saturation coverage, while at 205 °C, the white line intensity indicates 60% CO coverage. As observed for Pt/Al_2O_3, the CO coverage is lower under PROX reaction conditions, and is consistent with the observation that H_2 is competing with CO for Pt sites during the PROX reaction.

The XANES intensity also increases upon adsorption of hydrogen on the catalyst surface. The linear variation of the white line intensity with the amount of adsorbed hydrogen can be used to estimate the degree of hydrogen coverage [24]. The reduced catalysts without adsorbed and fully saturated with hydrogen were used as XANES references to estimate intermediate H_2 surface coverage (Table 4). Note that although the Nb catalysts adsorb H_2, Pt–O bonds are still observed by EXAFS. Further increase in temperature leads to 90% H_2 saturation at 110 °C and total H_2 desorption at 205 °C. These results indicate that while H_2 competes for adsorption sites with CO, at high temperature, there is little chemisorbed hydrogen.

In summary, the EXAFS results show that on the *unpromoted* Pt/Al_2O_3 only metallic Pt is present under PROX reaction conditions. On the *promoted* catalysts with *low* Nb loadings, EXAFS indicates the presence of only partially reduced Pt, while a portion of the Pt remains partially oxidized as PtO. On these catalysts, adsorption of H_2 competes with CO adsorption leading to lower CO coverage in the presence of H_2. Due to X-ray absorption by the niobia support, transmission XAS experiments could not be conducted on Pt supported on niobia.

3.3. Transmission infrared results

The catalysts were also analyzed by *operando* transmission FTIR and *in situ* DRIFTS under various conditions. Although the flow patterns and mass of catalysts were different between these IR reactors and the flow tubular reactor in which activity was measured, the conversions followed similar trends.

3.3.1. PROX reaction

Operando transmission FTIR spectra of Pt/Al_2O_3, Pt/5%Nb–Al_2O_3, and Pt/Nb_2O_5 catalysts were obtained under PROX reaction conditions (0.8% CO, 0.8% O_2, and 51% H_2, balance He) and at dif-

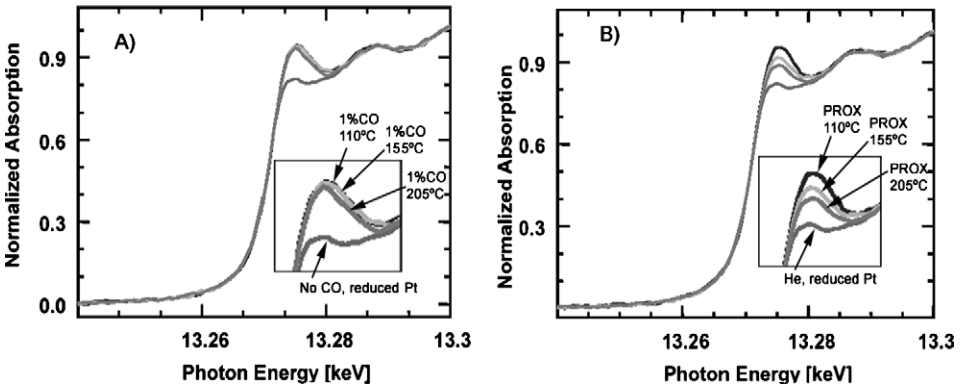

Fig. 1. Normalized L_{II} XANES spectra for the reduced Pt/Al_2O_3 catalyst at 110, 155, and 205 °C under: (A) flowing 1% CO balance He, and (B) PROX conditions: 0.8% CO, 0.8% O_2, and 4% H_2 balance He. The inserts are a magnified section where the normalized absorption is maximum.

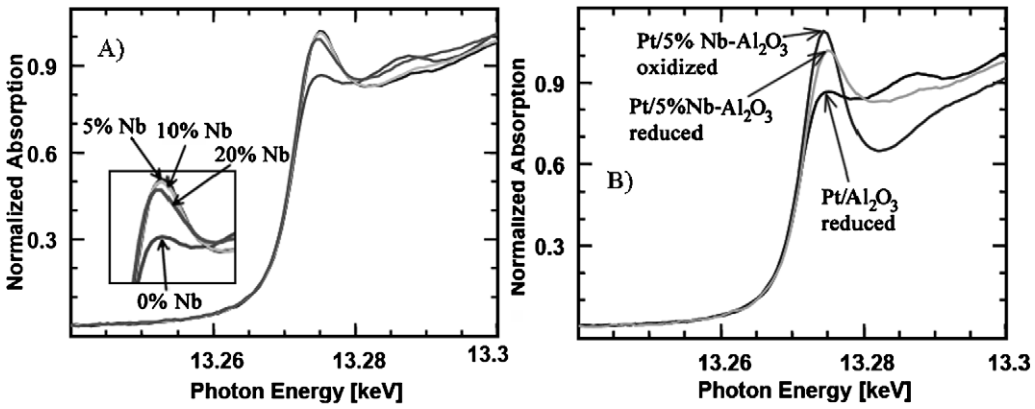

Fig. 2. Normalized L_{II} XANES spectra: (A) Pt/X%Nb–Al_2O_3 catalysts (X = 0, 5, 10, 20) in flowing He after being reduced at 250 °C, and (B) Pt/5%Nb–Al_2O_3 and Pt/Al_2O_3 catalyst reduced at 250 °C and oxidized at 205 °C. The insert in (A) shows the area were the normalized absorption is maximum.

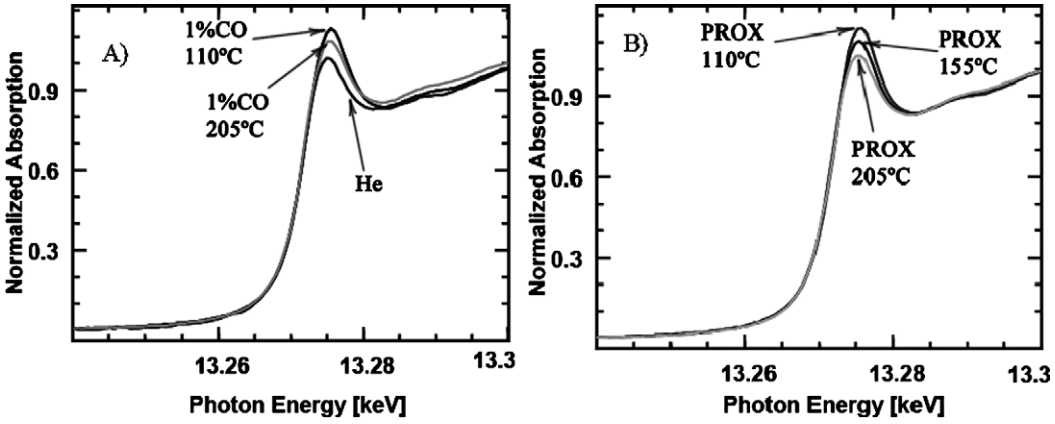

Fig. 3. Normalized L_{II} XANES spectra for the reduced Pt/5%Nb–Al_2O_3 catalyst from 13.24 to 13.30 keV. Spectra taken in: (A) flowing 1% CO balance He, and (B) PROX conditions: 0.8% CO, 0.8% O_2, and 4% H_2 balance He.

ferent temperatures. Conversions were measured at steady state by online gas chromatography. The IR spectra of linear CO (L–CO) adsorbed in the presence of hydrogen (not shown) were broad and located at 2036, 2018 and 2071 cm^{-1} on Pt/Al_2O_3, Pt/5%Nb–Al_2O_3 and Pt/Nb_2O_5 respectively. Adsorbed CO IR spectra under PROX reaction conditions (Fig. 4), were different than in pure CO flow showing additional bands appearing from 1700 to 1200 cm^{-1}. The new bands are attributed to formates (HCO_2^-) at 1590, 1393 and 1373 cm^{-1}, carbonates (CO_3^{2-}) at 1510 cm^{-1}, and bicarbonates (HCO_3^-) at 1645, 1440 and 1230 cm^{-1} [7,25–35] adsorbed on the supports. Fig. 4A shows the IR spectra on Pt/Al_2O_3 in the temperature range of 50–200 °C, along with the corresponding CO conversion at each temperature. At 50 °C, the L–CO band is located at 2052 cm^{-1} and gradually red-shifts to 2035 cm^{-1} at 200 °C (and a conversion of 15%). A small broad band corresponding to bridge bonded CO species is observed at 1819 cm^{-1} and its intensity decreases slightly as temperature increases. Adsorbed formate species give rise to an IR absorption band at 1591 cm^{-1} [7], which appears around 120 °C and increases with temperature and increasing CO conversion. A double peak observed at 1392 and 1373 cm^{-1} associated with formates also increases in intensity with temperature. Similar bands positions are shown in Fig. 4B for the Pt/5%Nb–Al_2O_3 catalyst, although at the same temperatures, CO conversions were higher than on Pt/Al_2O_3, consistent with the increase rates of reaction measured in the recycle reactor [17]. At higher conversions, the formate bands at 1589 cm^{-1}, 1373 cm^{-1} and carbonate bands are more intense on Pt/5%Nb–Al_2O_3 than on Pt/Al_2O_3. Such accumulation of surface formates on a Pt/Al_2O_3 catalyst under PROX reaction was also reported by Schubert et al. [7]. The absorption frequency of water is located at 1600 cm^{-1}, and its rotational–vibrational modes appear as a noise-like baseline around that frequency.

The IR spectra of Pt/Nb_2O_5, Fig. 4C, shows a lower L–CO absorbance, due to its lower dispersion, and no formates are observed with only adsorbed bicarbonates appearing at 1619 and 1414 cm^{-1}. These bands on Pt/Nb_2O_5 are about 26 cm^{-1} lower than those on Pt/Al_2O_3. The weak band at 2078 cm^{-1} corresponding to CO adsorbed on Pt^{2+}, remains almost unchanged as temperature increases, indicating no change in the CO surface coverage with increasing temperature, while for the Pt/Al_2O_3 and Pt/5%Nb–Al_2O_3 there is a decrease in CO coverage at high temperature. No bridge bonded CO was detected at any temperature and the (gas phase) CO_2 band for Pt/Nb_2O_5 was also much smaller than for the other catalysts in agreement with the lower activity of Pt/Nb_2O_5 towards CO oxidation during the PROX reaction [17]. The effluent from the reactor was analyzed in an IR gas-cell (1 in. OD, 6 in. long). For all the catalysts, the only PROX reaction products were water, CO_2, and CO gas.

3.3.2. CO oxidation only (without H_2)

Previously we reported that the selectivity to H_2 oxidation on Pt/Nb_2O_5 during the PROX reaction was favored whereas the CO_2 selectivity was drastically decreased, which is also shown in Table 1 [17]. *Operando* transmission FTIR for oxidation of CO in the *absence* of H_2 (0.8% CO and 0.8% O_2, balance He) was conducted on Pt/Nb_2O_5 and Pt/5%Nb–Al_2O_3 (Fig. 5).

The results show that on Pt/Nb_2O_5, the position of the L–CO band is 2083 cm^{-1}, slightly higher than during the PROX reaction. The intensity of the adsorbed CO band increases with in-

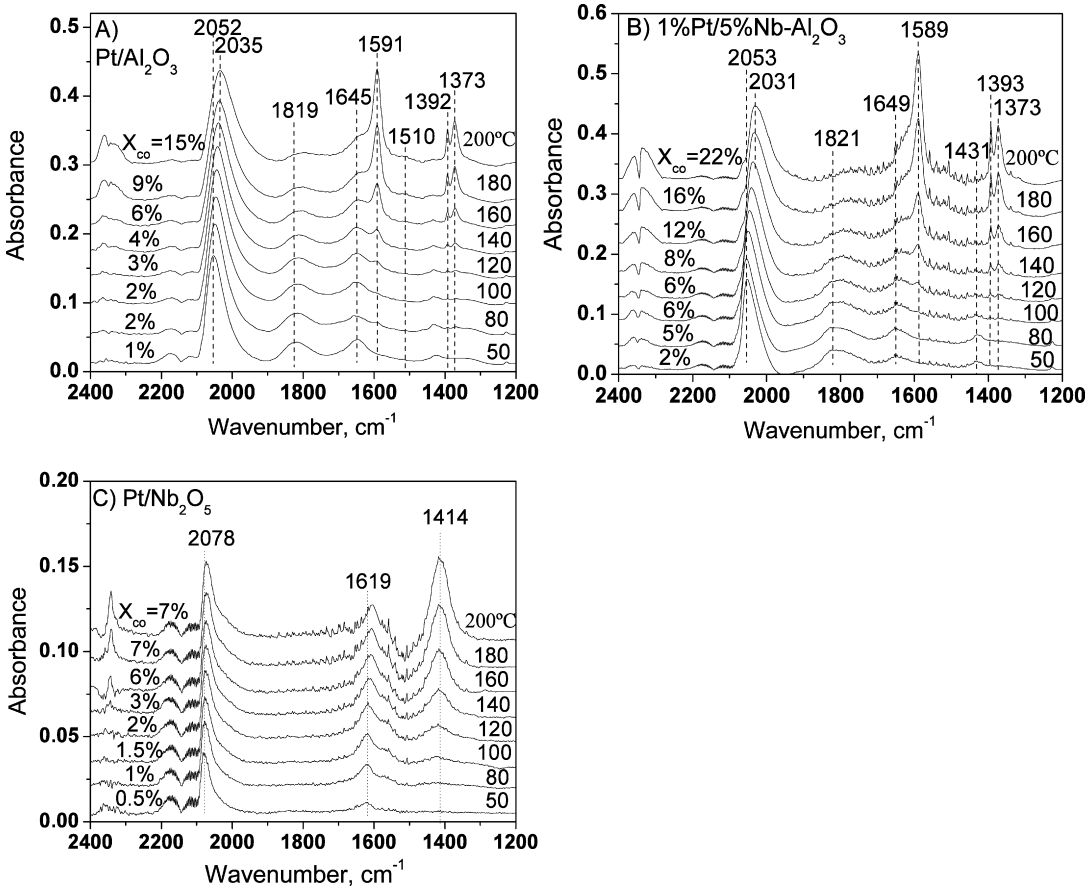

Fig. 4. FTIR spectra during PROX reaction conditions after reduction in H_2 at 250 °C for 1 h on (A) 1%Pt/Al_2O_3, (B) 1%Pt/5%Nb–Al_2O_3, and (C) 1%Pt/Nb_2O_5. Gas mixture: 0.8% CO, 0.8% O_2, 51% H_2, balance He. Total flow: 195 cc/min.

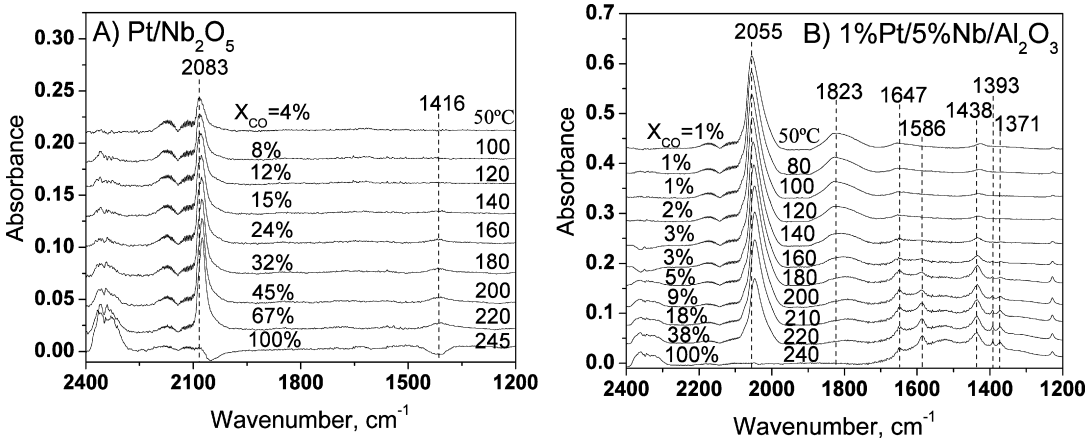

Fig. 5. FTIR spectra during the CO oxidation reaction after reduction in H_2 at 250 °C for 1 h on (A) 1%Pt/Nb_2O_5, and (B) 1%Pt/5%Nb–Al_2O_3, gas.0.8% CO, 0.8% O_2, balance He. Total flow: 195 cc/min.

creasing temperature before ignition. The increased intensity may indicate some oxidation of the reduced Pt under reaction conditions (Fig. 5A) since the position of the CO band does not change. For Pt/5%Nb–Al_2O_3 the frequency of the L–CO band is 2055 cm^{-1}, significantly higher than the main CO only adsorption band (2018 cm^{-1}). The higher frequency IR absorption band is assigned to CO adsorption on oxidized Pt. With increasing temperature, the CO IR absorption slowly decreases with increasing temperature consistent with the XANES spectra. On the Pt/Nb_2O_5 catalyst, there is only a very small bicarbonate band at 1416 cm^{-1}; while on Pt/5%Nb–Al_2O_3 there are a set of bands corresponding to formates at 1586, 1393, and 1371 cm^{-1}, and bicarbonates at 1647, and 1438 cm^{-1}. Other adsorbed carbonates species on Pt/Nb_2O_5 were not observed due to the low intensity of those bands. The band at 1416 cm^{-1} is absent on the Pt/Nb_2O_5 catalyst after ignition, Fig. 5A. CO ignition is observed at 245 and 240 °C for the Pt/Nb_2O_5 and Pt/5%Nb–Al_2O_3 catalysts, respectively. For Pt/5%Nb–Al_2O_3, Fig. 5B, the bands at 1647 (bicarbonate), 1586 (formate), 1438 (bicarbonate), 1393 (formate), and 1371 cm^{-1} (formate) are still present after ignition. However, these bands disappeared when oxygen alone was passed over the catalysts at the ignition temperature (not shown).

In summary, *operando* transmission FTIR spectra for CO oxidation show adsorbed CO only, very different than during the PROX

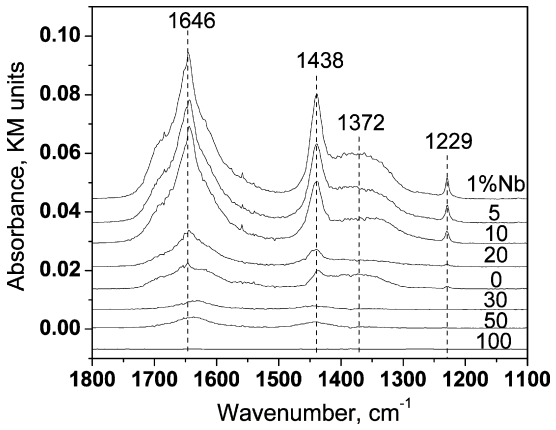

Fig. 6. CO_2 adsorption on Pt/X%Nb–Al_2O_3 catalysts (X = 1, 5, 10, 20, 30, 50, and 100%, X = 0 corresponds to the unpromoted Pt/Al_2O_3 catalyst). The adsorption was carried out at 50 °C after reduction at 200 °C in H_2.

reaction wherein additional bands ascribed to carbonates and formates are detected. The band of adsorbed L–CO appears at higher wave numbers on Pt/Nb_2O_5 than on promoted and unpromoted catalysts, indicating that the Pt surface is mainly populated by weakly adsorbed linear CO on semi-oxidized platinum. The presence or Pt^{2+} under reducing conditions as shown previously by the EXAFS/XANES results, does not inhibit the adsorption of CO in semi-oxidized platinum and neither the CO oxidation activity of the promoted catalyst. However, in the absence of hydrogen the Pt/Nb_2O_5 catalyst shows a CO ignition similar to that of Pt/5%Nb–Al_2O_3.

3.4. Diffuse reflectance (DRIFTS) FTIR

DRIFTS experiments were conducted to probe the state of the Nb=O species and to investigate the spectra of adsorbed CO_2 which originated bands in the 1800–1100 cm^{-1} range similar to the ones observed during the PROX reaction.

3.4.1. CO_2 adsorption

It is well known that CO_2 can form a variety of adsorbates on hydroxylated Al_2O_3 [32–35,40–44], therefore we studied its adsorption using DRIFTS. The catalysts were first reduced in H_2 at 200 °C for 1 h and then cooled to 50 °C, followed by introduction of CO_2 at that temperature. The DRIFTS results are presented in Fig. 6 for all the catalysts in terms of Kubelka–Munk units (KM) versus frequency in the range of 1800 to 1100 cm^{-1} on catalysts with different Nb loadings. It can be seen that on most catalysts CO_2 adsorption gives a set of bands similar to those observed under PROX conditions. The peaks observed in Fig. 6 are the superposition of absorbance bands from different species: bicarbonates at 1646, 1438, 1229 cm^{-1}, and formates at 1372 cm^{-1}. The shoulder near 1700 cm^{-1} on catalysts with low Nb loadings indicates the possible formation of carbonates [33]. It is readily observed that the catalysts loaded with 1, 5, and 10% Nb exhibit the highest intensities due to bicarbonates which decreases as loading increases and no bands are detected on Pt/Nb_2O_5.

The catalyst promoted with 20% Nb does not show a band at 1372 cm^{-1} (formate), whereas such band is still observed on Pt/Al_2O_3. While formates and carbonates appeared in the PROX oxidation on promoted and unpromoted Pt, the intensity is much higher than during the CO_2 adsorption experiment even though CO_2 concentrations are much lower during the PROX *operando* studies. Carbonates are seen only at high conversion during CO oxidation and none is detected on Pt/Nb_2O_5. So the formation of the low frequency bands observed during the PROX reaction is not only due to CO_2 adsorption on the support but also due to species generated during reaction, i.e. in the presence of hydrogen and formation of H_2O.

3.4.2. Nb=O infrared absorbance

Burcham et al. [37] using Raman and IR, studied the Nb=O symmetric stretching mode of Nb_2O_5 supported in different oxides. They found that Nb=O absorbed at 980 cm^{-1} when Nb_2O_5 was supported either on Al_2O_3 or TiO_2. We monitored the Nb=O band using DRIFTS after reducing the catalysts in H_2 200 °C for 1 h, then cooling to room temperature in He. Spectra were collected at room temperature and the spectrum of Pt/Al_2O_3 was subtracted from each spectra of the Nb promoted Pt/Al_2O_3 catalysts.

Fig. 7A shows the frequency of the Nb=O absorption band with increasing Nb loading, and Fig. 7B shows the normalized integrated intensity (IA) of the Nb=O band vs Nb loading (highest integrated area used as normalization factor). The absorption frequency of the Nb=O band shifts to higher values as Nb loading increases, leveling off at 980 cm^{-1} at the higher loadings (Fig. 7A), whereas the normalized intensity of the Nb=O absorption band increases with the Nb loading (Fig. 7B). It has been reported that when Nb=O coverage is exceeded, polymerization of Nb occurs [17,38,39]. The change in the Nb=O frequency together with the increase in its integrated absorbance, suggest that polymerization of finely dispersed Nb species occurs as Nb loading increases.

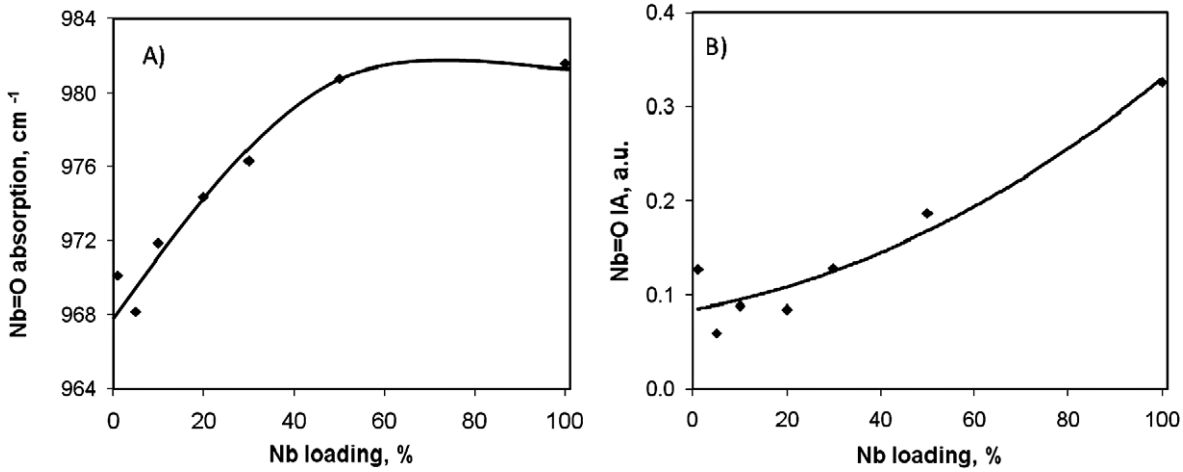

Fig. 7. DRIFTS on the Pt/X%Nb–Al_2O_3 (X = 0, 1, 5, 10, 20, 30, 50, and 100%) catalysts. (A) Change in the absorption frequency of the Nb=O bond as a function of Nb loading. (B) Relative integrated absorbance from (A).

4. Discussion

Activity results show that on Pt supported catalysts, hydrogen oxidation only is the fastest reaction igniting at room temperature, whereas during the PROX reaction CO inhibits hydrogen and oxygen dissociative adsorption at low temperature favoring CO_2 selectivity. As temperature increases, CO desorption increases, oxygen adsorption increases leading to hydrogen oxidation and a decrease in CO_2 selectivity. CO inhibition is further promoted by the presence of niobia at low concentration, but it decreases as niobia loading increases. On Pt/Nb_2O_5, however, CO adsorption is lower and weaker inhibiting less H_2 adsorption and oxidation resulting in low CO_2 selectivity. Interestingly on this catalyst CO oxidation is high when H_2 is not present. Below we attempt to correlate these activity-selectivity results with structural and FTIR results.

The EXAFS results show that, under PROX reaction conditions, on the unpromoted Pt/Al_2O_3 only metallic Pt is present, while on catalysts promoted with low Nb loadings, the Pt is partially reduced with some partially oxidized Pt^{2+}. The presence of Pt^{2+} under reducing conditions, as shown by EXAFS/XANES, does not inhibit the adsorption of CO on semi-oxidized platinum. It is likely that these oxidized Pt species play a role on increasing the CO_2 selectivity under PROX reaction, thus explaining the promoting effect of Nb.

The presence of semi-oxidized Pt on the promoted catalysts suggests a complex surface made of Pt crystallites and PtO species affected by niobia moieties surrounding the Pt crystallites or decorating them. IR results indicate that Nb moieties can have different structural characteristics depending on loading. The lower frequency Nb=O band observed during the DRITFS experiments on low Nb loadings catalysts indicates formation of isolated Nb=O moieties. As the Nb loading increases, two-dimensional Nb islands appear and thus the intensity of Nb=O increases. Above the monolayer coverage (20%), the frequency of Nb=O remains constant at 980 cm^{-1} which is consistent with the presence of Nb_2O_5 aggregates [36,37]. In our previous work, we reported that *ex situ* XPS showed an abrupt increase in the Nb 3d binding energy when the Nb loading reached a monolayer coverage, also indicative of the formation of three-dimensional bulk niobia oxide at higher Nb loadings [17]. This structural change is in agreement with the blue shift of the Nb=O absorption frequency observed in Fig. 6A. Under these conditions several scenarios can develop with Nb moieties in close proximity to the Pt crystallites, or decorating them at high loadings or both.

Increasing the loading of Nb changes the support environment and it is expected that such changes will also affect the interaction between Pt and the reacting species. The niobia-support interaction has been discussed in the literature [45–49], indicating that support surface hydroxyls play a fundamental role in the type of species formed. The formation of Nb species on the Al_2O_3 support not only occurs by impregnation of the support, but it also occurs by titration of surface hydroxyls [50]. It is not clear how these support hydroxyls affect the reaction however. DRIFTS spectra of the various supports after reduction (not shown), showed broad bands between 3700 and 2750 cm^{-1} corresponding to surface hydroxyls and chemisorbed water, which varied with Nb loading. A possible effect of the niobia support is that hydrogen adsorbed on Pt can spillover to the support [26,52–56] and react with the support hydroxyls [51,53,57]. Therefore a lower concentration of hydroxyls, caused by niobia titration, could decrease hydrogen oxidation and favor CO_2 selectivity. In fact, Pedrero et al. [10] found that adding Cs progressively to Pt supported catalysts titrated surface hydroxyls, which improved the PROX selectivity by restricting the hydrogen spill-over pathway. We have no evidence that spillover occurs on our catalysts, however, and we cannot ascertain its role in the activity/selectivity results obtained in our catalysts, but this pathway cannot be completely ruled out either.

No significant differences were observed between the *operando* PROX-IR spectra of L–CO on Pt/Al_2O_3 and $Pt/5\%Nb–Al_2O_3$ catalysts (Fig. 4). This further supports the hypothesis that the partially oxidized Pt species increase the oxidation of CO favoring CO_2 selectivity, although how this pathway take place is not known. There is a significant difference in both intensity and frequency of the CO spectra on Pt/Nb_2O_5, a catalyst with low CO_2 selectivity. CO absorbance is smaller, consistent with the lower dispersion of Pt on this catalyst, and the L–CO frequency is higher, indicating a weaker bond onto a more oxidized surface. Thus one possibility to explain the low CO_2 selectivity of Pt/Nb_2O_5 is that this weakly adsorbed CO does not inhibits the rate of H_2 and oxygen dissociative adsorption, resulting in higher hydrogen oxidation and lower CO_2 selectivity. We hypothesize that the additional species formed in the presence of hydrogen during the PROX reaction, are responsible for the decrease in both amount and strength of CO adsorption decreasing its inhibition of hydrogen oxidation.

FTIR spectra during the PROX reaction show several additional bands corresponding to formates and bicarbonates. The CO_2 adsorption DRIFTS experiments show that bicarbonate and carbonates bands also appear, indicating that the additional carbonate and formate species could originate from CO_2 formed during CO oxidation. The intensity of the formate band produced from water and CO_2 during the *operando* PROX FTIR experiments increase with conversion. While band intensities in transmission and KM-units in DRIFTS experiments are similar but not completely equivalent, the intensity of these low frequency bands is larger during the PROX reaction even though CO_2 concentration is lower. This suggests that the carbonate, bicarbonate and formate bands cannot be ascribed only to CO_2 adsorbed on the support, and that the reaction pathway is not just the simple competitive adsorption and reaction between adsorbed CO, hydrogen, and oxygen. Additional species related to these low frequency bands must also form from the adsorbed reactants. The formation of hydroxyls both, on Pt, and the support are known to play a role. In fact detailed kinetics simulations of the PROX reaction in our group indicate that the rate of formation of adsorbed hydroxyls is the fastest one followed by its reaction with adsorbed hydrogen to form water and with adsorbed CO to form CO_2 [58]. These adsorbed hydroxyls can form other species with adsorbed CO that might be responsible for the low frequency bands observed during the PROX reaction. We speculate that these additional species may play a role in reducing CO adsorption and its inhibition of H_2 oxidation on Pt/Nb_2O_5. In the *operando* CO oxidation only FTIR experiments, very small low frequency bands are detectable on $Pt/5\%Nb–Al_2O_3$, while there are no such bands on the Pt/Al_2O_3 catalyst. Thus, in the absence of hydrogen, these additional species are not present and CO readily adsorbs on semi-oxidized Pt and form CO_2 at a rate comparable to Pt/Al_2O_3 which explains why during CO oxidation only is high on Pt/Nb_2O_5 but low during the PROX reaction.

5. Conclusion

The present work combines XAFS and IR characterization techniques to better understand the promotion effect of Nb on Pt/Al_2O_3 catalysts for the PROX reaction. Addition of small amounts of Nb (<5%) stabilizes 40% of the loaded platinum as Pt^{2+} even after reduction treatments. Increasing loadings of Nb forms NbO_x species that first forms isolated islands, then a monolayer, and three-dimensional oxides at very high loadings. These NbO_x species may be surrounding the Pt crystallites affecting the interface between Pt and the alumina support and the species adsorbed on these metal–support interfaces. In addition, some Nb may be decorating the Pt surface affecting the oxidation state. These interactions are

complex, thus it is difficult to ascertain uniquely which factors are responsible for the changes in the observed activity and selectivity. Nonetheless it is clear that the formation of partially oxidized Pt species increases CO_2 activity and selectivity.

The PROX reaction involves both CO and H_2 oxidation as well as the formation of intermediates associated with the presence of hydroxyls, CO_2 and H_2O on the catalyst's surface. Adsorbed CO inhibits the much faster H_2 oxidation reaction and this effect increases with low Nb loading and the presence of partially oxidized Pt giving improved CO_2 selectivity. On Pt/Nb_2O_5 there is also some oxidized Pt, but the CO_2 selectivity during the PROX reaction is very low. It is suggested that the low CO_2 selectivity results from the decrease in the amount and strength of CO adsorption due to additional intermediate species. This decreases CO inhibition of hydrogen and oxygen adsorption thus favoring hydrogen oxidation. In the absence of hydrogen, these intermediates are not formed and the rate of CO oxidation only is much higher than during the PROX reaction on Pt/Nb_2O_5.

Acknowledgments

We gratefully acknowledge partial support of this work by a grant from Companhia Brasileira de Metalurgia e Mineração, CBMM; a Bayer Postdoctoral Fellowship in Environmental Chemistry through the Center for Environmental Science and Technology at the University of Notre Dame, and NSF Grant CTS 0138070. Use of the Advanced Photon Source was supported by the US Department of Energy, Office of Basic Energy Sciences, Office of Science (DOE-BES-SC), under Contract No W-31-109-Eng-38. The MRCAT is funded by the member institutions and DOE-BES-SC under contracts DE-FG02-94ER45525 and DE-FG02-96ER45589.

References

[1] J.C. Amphlett, M.J. Evans, R.F. Mann, R.D. Wier, Can. J. Chem. Eng. 63 (1985) 605.
[2] E. Santacesaria, S. Carra, Appl. Catal. 5 (1983) 345.
[3] S.H. Oh, R.M. Sinkevitch, J. Catal. 142 (1993) 254.
[4] O.S. Alexeev, S.Y. Chin, M.H. Engelhard, L. Ortiz-Soto, M.D. Amiridis, J. Phys. Chem. B 109 (2005) 23430.
[5] M.M. Schubert, M.J. Kahlich, H.A. Gasteiger, R.J. Behm, J. Power Sources 84 (1999) 175.
[6] M.M. Schubert, M.J. Kahlich, G. Feldmeyer, M. Hüttner, S. Hackenberg, H.A. Gasteiger, R.J. Behm, Phys. Chem. Chem. Phys. 3 (2001) 1123.
[7] M.M. Schubert, H.A. Gasteiger, R.J. Behm, J. Catal. 172 (1997) 256.
[8] M.J. Kahlich, H.A. Gasteiger, R.J. Behm, J. Catal. 171 (1997) 93.
[9] D.H. Kim, M.S. Lim, Appl. Catal. A 224 (2002) 27.
[10] C. Pedrero, T. Waku, E. Iglesia, J. Catal. 233 (2005) 242.
[11] M. Brown, A. Green, US Patent 3 088 919, Engelhard Industries Inc., 1963.
[12] C. He, H.R. Kunz, J.M. Fenton, J. Electrochem. Soc. 148 (2001) A1116.
[13] D. Tibiletti, E.A.B. d. Graaf, S.P. Teh, G. Rothenberg, D. Farrusseng, C. Mirodatos, J. Catal. 225 (2004) 489.
[14] A. Wootsch, C. Descorme, D. Duprez, J. Catal. 225 (2004) 259.
[15] C. Kwak, T.-J. Park, D.J. Suh, Appl. Catal. A 278 (2005) 181.
[16] Y. Minemura, S.-i. Ito, T. Miyao, S. Naito, K. Tomishige, K. Kunimori, Chem. Commun. 11 (2005) 1429.
[17] S. Guerrero, J.T. Miller, E.E. Wolf, Appl. Catal. A 328 (2007) 27.
[18] C.U. Segre, N.E. Leyarovska, L.D. Chapman, W.M. Lavender, P.W. Plag, A.S. King, A.J. Kropf, B.A. Bunker, K.M. Kemner, P. Dutta, R.S. Duran, J. Kaduk, in: Synchrotron Radiation Instrumentation, 11th US National Conference, 2000.
[19] T. Ressler, J. Synchrotron Radiat. 5 (1998) 118.
[20] F.W. Lytle, D.E. Sayers, E.A. Stern, Physica B 158 (1989) 701.
[21] R.B. Greegor, F.W. Lytle, J. Catal. 63 (1980) 476.
[22] Y. Notoya, K. Hayakawa, T. Fujikawa, T. Kubota, T. Shido, K. Asakura, Y. Iwasawa, Chem. Phys. Lett. 357 (2002) 365.
[23] T. Kubota, K. Asakura, Y. Iwasawa, Catal. Lett. 46 (1997) 141.
[24] T. Kubota, K. Asakura, N. Ichikuni, Y. Iwasawa, Chem. Phys. Lett. 256 (1996) 445.
[25] L.-C. de Ménorval, A. Chaqroune, B. Coq, F. Figueras, J. Chem. Soc. Faraday Trans. 93 (1997) 3715.
[26] E.V. Benvenutti, L. Franken, C.C. Moro, Langmuir 15 (1999) 8140.
[27] J. Oudar, H. Wise, Deactivation and Poisoning of Catalysts, Dekker, New York, 1985.
[28] M. Primet, J. Catal. 88 (1984) 273.
[29] L.C. de Ménorval, A. Chaqroune, B. Coq, F. Figueras, J. Chem. Soc. Faraday Trans. 93 (1997) 3715.
[30] R.G. Greenler, K.D. Burch, K. Kretzschmar, R. Klauser, A.M. Bradshaw, B.E. Hayden, Surf. Sci. 152–153 (1985) 338.
[31] P.-A. Carlsson, L. Osterlund, P. Thormahlen, A. Palmqvist, E. Fridell, J. Jansson, M. Skoglundh, J. Catal. 226 (2004) 422.
[32] C. Morterra, G. Magnacca, Catal. Today 27 (1996) 497.
[33] D.G. Rethwisch, J.A. Dumesic, Langmuir 2 (1986) 73.
[34] J. Baltrusaitis, J.H. Jensen, V.H. Grassian, J. Phys. Chem. 110 (2006) 12005.
[35] M.-I. Baraton, X. Chen, K.E. Consalves, Nanostruct. Mater. 8 (1997) 435.
[36] H. Hosoda, T. Tabaru, S. Semboshi, S. Hanada, J. Alloys Compd. 281 (1998) 268.
[37] L.J. Burcham, J. Datka, I.E. Wachs, J. Phys. Chem. 103 (1999) 6015.
[38] J.M. Jehng, I.E. Wachs, J. Mol. Catal. 67 (1991) 369.
[39] T. Tanaka, T. Yoshida, H. Yoshida, H. Aritani, T. Funabiki, S. Yoshida, J.-M. Jehng, I.E. Wachs, Catal. Today 28 (1996) 71.
[40] J.C. Lavalley, Catal. Today 27 (1996) 377.
[41] Z. Gandao, B. Coq, L.C. de Ménorval, D. Tichit, Appl. Catal. A 147 (1996) 395.
[42] S.U. Rege, R.T. Yang, Chem. Eng. Sci. 56 (2001) 3781.
[43] M. Casarin, D. Falcomer, A. Glisenti, A. Vittadini, Inorg. Chem. 42 (2003) 436.
[44] M.A. Abdel-Rehim, A.C.B. dos Santos, V.L.L. Camorim, A. da Costa Faro Jr., Appl. Catal. A 305 (2006) 211.
[45] I.E. Wachs, Catal. Today 27 (1996) 437.
[46] S.M. Maurer, D. Ng, E.I. Ko, Catal. Today 16 (1993) 319.
[47] X. Gao, I.E. Wachs, M.S. Wong, J.Y. Ying, J. Catal. 203 (2001) 18.
[48] P.A. Burke, E.I. Ko, J. Catal. 129 (1991) 38.
[49] S.M. Maurer, E.I. Ko, Catal. Lett. 12 (1992) 231.
[50] I.E. Wachs, J.M. Jehng, G. Deo, H. Hu, N. Arora, Catal. Today 28 (1996) 199.
[51] H. Knözinger, P. Ratnasamy, Catal. Rev. Sci. Eng. 17 (1978) 31.
[52] M.A. Vannice, J. Mol. Catal. 59 (1990) 165.
[53] M. Vaarkamp, J.T. Miller, F.S. Modica, D.C. Koningsberger, J. Catal. 163 (1996) 294.
[54] P. Sermon, G.C. Bond, J. Chem. Soc. Faraday Trans. 76 (1980) 889.
[55] R. Kramer, M. Andre, J. Catal. 58 (1979) 287.
[56] S.J. Techner, A.R. Mazabrard, G. Pajonk, G.E.E. Gardes, C. Hoang-Van, J. Colloid Interface Sci. 58 (1977) 88.
[57] W.J. Ambs, M.M. Mitchell, J. Catal. 82 (1983) 226.
[58] S. Guerrero, Ph.D. thesis, University of Notre Dame, 2007.